

## HEMATOPOIESIS AND STEM CELLS

**Bcl2 overexpression rescues the hematopoietic stem cell defects in Ku70-deficient mice by restoration of quiescence**

Yulan Qing, Zhengqi Wang, Kevin D. Bunting, and Stanton L. Gerson

Case Comprehensive Cancer Center, National Center for Regenerative Medicine, Seidman Cancer Center, University Hospitals Case Medical Center and Case Western Reserve University, Cleveland, OH

**Key Points**

- Loss of Ku70 results in loss of HSC quiescence, which correlates with loss of HSC maintenance.
- Bcl2 overexpression rescues HSC defects in Ku70<sup>-/-</sup> mice by restoring quiescence, without restoration of DNA repair capacity.

**DNA repair is essential for hematopoietic stem cell (HSC) maintenance. Ku70 is a key component of the nonhomologous end-joining pathway, which is the major pathway for DNA double-strand break repair. We find that HSCs from Ku70-deficient mice are severely defective in self-renewal, competitive repopulation, and bone marrow (BM) hematopoietic niche occupancy and that loss of quiescence results in a dramatic defect in the maintenance of Ku70-deficient HSCs. Interestingly, although overexpression of Bcl2 does not rescue the severe combined immunodeficiency phenotype in Ku70-deficient mice, overexpression of Bcl2 in Ku70-deficient HSCs almost completely rescued the impaired HSC quiescence, repopulation, and BM hematopoietic niche occupancy capacities. Together, our data indicate that the HSC maintenance defect of Ku70-deficient mice is due to the loss of HSC quiescent populations, whereas overexpression of Bcl2 rescues the HSC defect in Ku70-deficient mice by restoration of quiescence. Our study uncovers a novel role of Bcl2 in HSC quiescence regulation. (*Blood*. 2014;123(7):1002-1011)**

**Introduction**

Genomic integrity is essential for organism development and longevity and has recently been recognized as critical for the maintenance of stem cell populations.<sup>1-5</sup> Eukaryotic cells maintain genomic integrity by utilizing multiple DNA repair pathways,<sup>6</sup> and emerging evidence supports the hypothesis that DNA repair is also crucial for maintaining hematopoietic stem cell (HSC) function.<sup>7</sup>

HSC function is closely coupled to the cells' unique cell-cycle kinetics, in which adult HSCs are predominantly quiescent, undergoing proliferation in response to stress. Increased proliferation or loss of quiescence in HSCs correlates with loss of HSC function.<sup>8-11</sup> Although a variety of molecules regulate HSC quiescence,<sup>12-14</sup> DNA-repair pathways have not been implicated in HSC quiescence regulation directly.

DNA double-strand breaks (DSBs) are perhaps the most harmful type of DNA damage. DSBs can be induced by ionizing radiation, the byproducts of cellular metabolism (reactive oxygen species), or during V(D)J recombination in T and B lymphocytes.<sup>15</sup> Mammalian cells employ 2 major mechanisms for DSB repair: homologous recombination (HR) and nonhomologous end-joining (NHEJ).<sup>16,17</sup> HR can be error-free and is only operative in the S/G<sub>2</sub> phases of the cell cycle when a sister chromatid is available. NHEJ is error-prone and functions in all phases of the cell cycle. When a DSB occurs, the broken ends are held in close proximity by the Ku70-Ku80 heterodimer and DNA-dependent protein kinase catalytic subunit (DNA-PK<sub>cs</sub>), forming the DNA-dependent protein kinase (DNA-PK) complex. The kinase activity of the DNA-PK complex is activated by Artemis nuclease and the repair process is completed

by XRCC4–DNA ligase IV–mediated DNA ligation.<sup>18</sup> Defects in NHEJ result in marked sensitivity to ionizing radiation and immunodeficiency. In humans, 15% of severe combined immunodeficiency (SCID) cases are associated with inherited defects in NHEJ.<sup>19</sup> Mice deficient in NHEJ components are viable and hypersensitive to irradiation and show a SCID phenotype.<sup>20-24</sup>

NHEJ is the preferential repair mechanism in resting HSCs in response to DSBs.<sup>25</sup> NHEJ components are also required for HSC maintenance. Ku80-deficient HSCs have attenuated self-renewal and ultimately stem cell functional exhaustion.<sup>26</sup> Mice with a hypomorphic mutation in DNA ligase IV have diminished DSB repair activity and progressively lose HSCs during aging. In addition, HSCs with the hypomorphic Lig4<sup>Y288C</sup> mutation display increased proliferation and impaired maintenance.<sup>22</sup> However, the mechanism by which the NHEJ pathway regulates HSC function is not clear.

Bcl2 is a prototypical oncogene. It was discovered at the t(14;18) translocation breakpoint in human B-cell follicular lymphomas and overexpression of Bcl2 is one of the major oncogenic driver mechanisms in lymphomas and leukemias.<sup>27-29</sup> The antiapoptotic function of Bcl2 has been well established,<sup>30,31</sup> and the antiapoptotic function of Bcl2 in HSCs has also been demonstrated in Bcl2 transgenic mice, which have increased HSC pools and are resistant to irradiation.<sup>32,33</sup>

Overexpression of Bcl2 has also shown significant impact on proliferation. Overexpression of Bcl2 delays G<sub>0</sub>/1-S transition in T cells, and Bcl2-deficient T cells demonstrate accelerated cell-cycle progression.<sup>34</sup> In FDC-P1 cells following interleukin-3 withdrawal, Bcl2–expressing cells rapidly arrested in the G<sub>1</sub>/0 phase and were

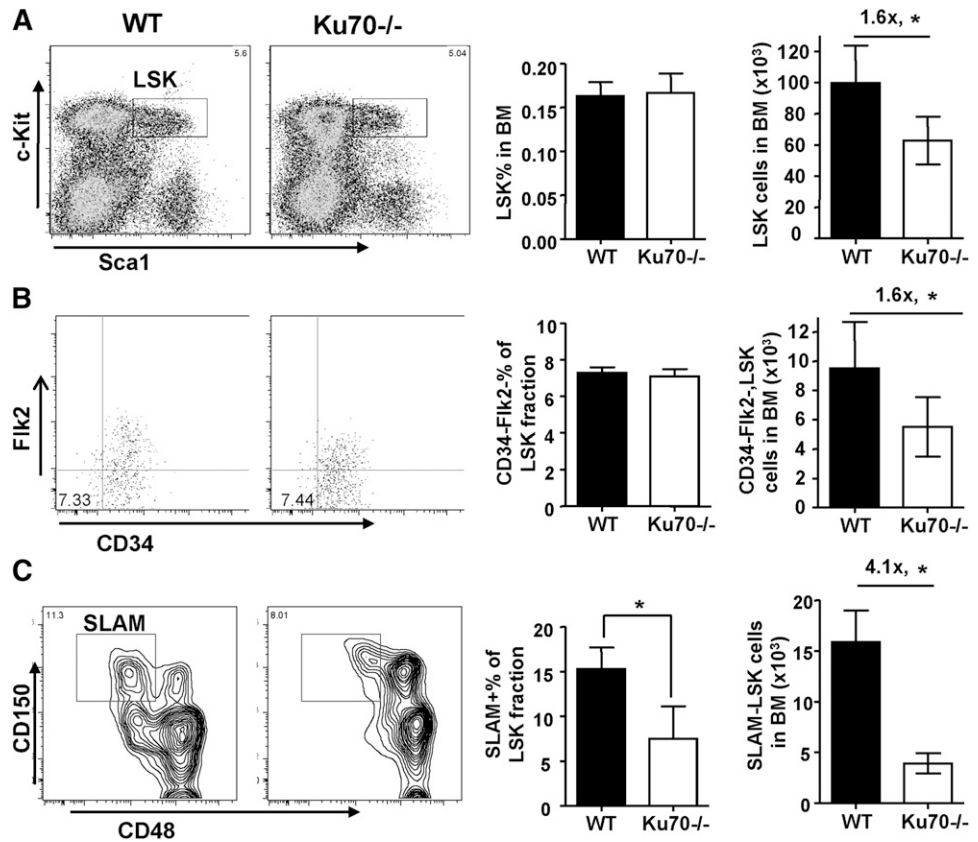
Submitted August 26, 2013; accepted December 19, 2013. Prepublished online as *Blood* First Edition paper, January 6, 2014; DOI 10.1182/blood-2013-08-521716.

The online version of this article contains a data supplement.

The publication costs of this article were defrayed in part by page charge payment. Therefore, and solely to indicate this fact, this article is hereby marked "advertisement" in accordance with 18 USC section 1734.

© 2014 by The American Society of Hematology

**Figure 1. Phenotypic characterization of HSC and progenitor compartment in *Ku70*<sup>-/-</sup> mice.** BM cells from 3-month-old *Ku70*<sup>-/-</sup> mice and WT littermates were assayed by multiparameter fluorescence-activated cell sorter (FACS) for proportion of HSC and progenitor populations. At least 6 mice per genotype were compared. Representative FACS pregated profiles of live, lineage-negative cells and frequencies of each indicated population are shown, and the absolute numbers of each population were calculated by multiplying the BM cell numbers with frequency. (A) Hematopoietic progenitors (*lin*<sup>-</sup>, *Sca1*<sup>+</sup>, *c-Kit*<sup>+</sup> [LSK]), (B) long-term HSCs (LT-HSCs) (LSK, *CD34*<sup>-</sup>, *Flk2*<sup>-</sup>), and (C) signaling lymphocyte activating molecule (SLAM)-LSK. Significance was determined by a 2-tailed Student *t* test. Error bars indicate the standard deviation (SD). \**P* < .05.



refractory to restimulation with interleukin-3.<sup>35</sup> Similarly, in NIH3T3 fibroblasts, *Bcl2* overexpression accelerates withdrawal into *G*<sub>0</sub> after growth factor deprivation and delays S-phase entry after restimulation with growth factors.<sup>36</sup> These findings suggest that *Bcl2* overexpression regulates cellular proliferation by controlling the *G*<sub>0</sub> to *G*<sub>1</sub> transition.<sup>37</sup> However, the antiproliferation function of *Bcl2* in HSCs has not been examined.

Here, we use *Ku70*-deficient mice as a model to examine the role of NHEJ in HSC quiescence, maintenance, and function and demonstrate that lack of *Ku70* results in loss of HSC quiescence. More interestingly, overexpression of *Bcl2* promotes HSC quiescence and rescues the HSC defects in *Ku70*-deficient mice.

## Methods

### Mice

The C57BL/6 (CD45.2), congenic strain B6.SJL-Ptpr<sup>a</sup>Pep3<sup>b</sup>/BoyJ (BoyJ, CD45.1), and transgenic green fluorescent protein (GFP) mice were obtained from The Jackson Laboratory. *Ku70*<sup>-/-</sup> mice were kindly provided by Dr Alt,<sup>21</sup> and transgenic *Bcl2* mice under H2-K promoter have been described previously.<sup>33</sup> All mice were housed in a specific-pathogen-free facility. Unless otherwise stated, all mice were studied between 8 and 16 weeks of age. All mouse studies were approved by the institutional animal care and use committee at Case Western Reserve University (Cleveland, OH).

### Hematology

Peripheral blood (PB) was obtained from the retro-orbital sinus using microcapillary tubes. For blood cell counts, the Coulter counter Z2 (Beckman Coulter, Fullerton, CA) was used. Bone marrow (BM) was harvested from

both hindlimbs (tibias and femurs) of mice, and total nucleated cell numbers were counted using a hemacytometer.

### Flow cytometry and cell sorting

Flow cytometry was performed on a BD LSRII or LSR II (BD Biosciences, San Jose, CA), and data were analyzed using FlowJo software (TreeStar, Ashland, OR). Antibodies included CD45.2, CD45.1, Ly-6G (Gr-1), CD11b (Mac-1), CD45R/B220, CD4 (L3T4), CD8 (Ly2), Ter119/Ly76, *Sca1* (Ly-6A/E), *c-Kit* (CD117), CD34, *Flk2*, CD48 (BD Bioscience), and CD150 (Biolegend).

BD Aria was used for cell sorting. BM cells were lineage depleted using a lineage-depletion kit (Miltenyi Biotec, Auburn, CA) and labeled with phycoerythrin (PE)-conjugated lineage antibodies, fluorescein isothiocyanate (FITC)-conjugated *Sca1*, and allophycocyanin (APC)-conjugated *c-Kit*, and LSK cells were sorted.

### Transplantation assay

For noncompetitive transplantation,  $2 \times 10^6$  whole BM cells from test mice were injected into lethally irradiated (11 Gy) BoyJ mice through the lateral tail vein. Then 16 to 24 weeks posttransplantation, recipients were used as donors for the subsequent transplantation cycle. For competitive transplantation,  $2 \times 10^6$  BM cells from mice with each genotype were mixed with the same number of wild-type (WT) competitor BM cells and transplanted into lethally irradiated BoyJ recipients. For nonmyeloablative transplantation,  $5 \times 10^6$  BM cells were infused into unconditioned recipients.

### Analysis of HSC cell cycle and proliferation

A total of  $5 \times 10^6$  BM cells were incubated in Iscove modified Dulbecco medium in the presence of 5  $\mu$ g/mL Hoechst 33342 at 37°C for 45 minutes and 1  $\mu$ g/mL pyronin Y for an additional 45 minutes. DNA and RNA contents within LSK and SLAM-LSK fractions were analyzed to determine the cell-cycle status.

Mice were treated through intraperitoneal injection of 1 mg 5-bromo-2'-deoxyuridine (BrdU; Sigma-Aldrich) per 10 g body weight and 1 mg/mL BrdU

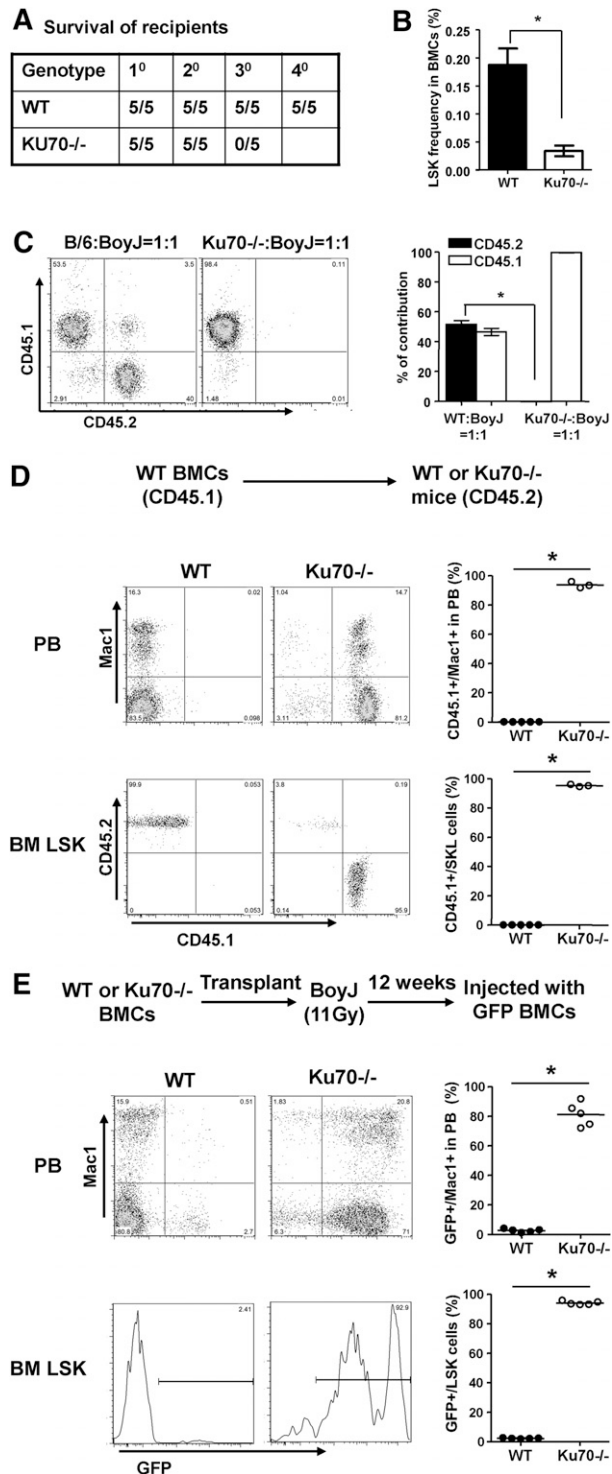


**Figure 2. Functional assessment of HSCs from Ku70<sup>-/-</sup> mice.** (A) Non-competitive serial transplants were initiated by transplanting  $2 \times 10^6$  whole BM pooled from 3-month-old WT ( $n = 3$ ) or Ku70<sup>-/-</sup> ( $n = 2$ ) donor mice (CD45.2) into irradiated recipients (CD45.1,  $n = 5$  per group). Secondary and tertiary transplants were performed after 16 to 24 weeks of engraftment by pooling BM from 3 to 4 reconstituted recipients to transplant  $2 \times 10^6$  whole BM into new groups of irradiated CD45.1 recipients. Survival of recipient mice was monitored. Shown is a representative result of 2 independent experiments. (B) Prior to transplant into tertiary recipients, BM from 5 secondary recipients of both genotypes was assayed by FACS for the frequency of LSK. Error bars indicated SD of the mean, and significance was determined by a 2-tailed Student *t* test.  $*P < .01$ . (C) BM from 3-month-old WT and Ku70<sup>-/-</sup> mice (CD45.2) was harvested and mixed with WT BM (CD45.1) at a 1:1 ratio and transplanted into lethally irradiated WT mice (CD45.1,  $n = 5$  per group). Then 16 weeks after transplantation, donor chimerism in the PB was analyzed and

was added to the drinking water for 30 hours. BrdU incorporation within gated LSK cells was evaluated using a BrdU staining kit (BD Biosciences).

### Apoptosis analysis and $\gamma$ H2AX analysis

BM cells were stained with PE-labeled lineage antibodies, APC-c-Kit, PE-Cy7-Sca-1, or APC-Cy7-labeled lineage and CD48 antibodies, APC-c-Kit, PE-Cy7-Sca1, and PE-CD150. Apoptosis rates within LSK or SLAM-LSK were determined by staining with FITC-annexin V (BD Biosciences) and 4',6'-diamino-2'-phenylindole (DAPI; Invitrogen).

$\gamma$ H2AX flow analysis were performed following the methods described previously.<sup>38</sup> BM cells were stained with APC-Cy7-labeled lineage and CD48 antibodies, APC-c-Kit, PE-Cy7-Sca1, and PE-CD150 and fixed and permeabilized before they were stained with  $\gamma$ H2AX antibody (Millipore).

### Quantitative PCR

RNA was isolated from sorted LSK cells using the PicoPure Kit (Invitrogen), and cDNA was prepared using the SuperScript III First Strand Synthesis system (Invitrogen) and analyzed in triplicate with FastStart Universal SYBR Green Master (Roche Diagnostics, Indianapolis, IN). Real-time polymerase chain reaction (PCR) was performed using the 7500 FAST real-time PCR system (Applied Biosystems, Foster City, CA). Specificity of products was confirmed by melting curve analysis and assessing band size in 2.5% agarose gels. Data were analyzed with 7500 Fast System Sequence Detection software (version 1.3.1).

### Statistical analysis

Where not otherwise stated, the Student *t* test was used to determine significance.

## Results

### Deficiency in Ku70 affects BM immunophenotypic HSC population at steady state

Ku70<sup>-/-</sup> mice were obtained through a Ku70 heterozygous cross. The yield of Ku70<sup>-/-</sup> mice was  $<5\%$  at weaning age (our unpublished results), indicating a growth and development disadvantage. At steady state, no difference was observed in hematocrit or red cell counts in PB, whereas Ku70<sup>-/-</sup> mice showed decreased white blood cell counts due to the lack of T and B lymphocytes (supplemental Table 1, available on the *Blood* Web site) and the calculated absolute cell numbers of myeloid cells (Mac1<sup>+</sup>) were compatible with those from WT mice (supplemental Figure 1A). Ku70<sup>-/-</sup> mice also showed reduced BM cellularity, probably due to significantly reduced body size (supplemental Figure 1B).<sup>21,39</sup>

The effects of Ku70 on the HSC/progenitor pool at steady state were also examined. The frequencies of LSK and LT-HSC were not significantly different (Figure 1A-B), whereas the frequency of

**Figure 2 (continued)** quantitated. Similar results were obtained in 3 independent experiments. Error bars indicate the SD, and significance was determined by a 2-tailed Student *t* test.  $*P < .005$ . (D) Three-month-old recipient mice (CD45.2) were transplanted with WT (CD45.1) BM cells without any ablative conditioning. Donor-derived Mac1<sup>+</sup> cells in the PB were analyzed 16 weeks after transplantation from 2 separate injections (WT,  $n = 5$ ; Ku70<sup>-/-</sup>,  $n = 3$ ). Then 16 to 24 weeks after transplantation, BM cells were isolated from recipient mice and chimerism of LSK population in each recipient mouse was analyzed. (E) A total of  $5 \times 10^6$  BM cells from WT, Ku70<sup>-/-</sup> (CD45.2) donors were transplanted into lethally irradiated WT (CD45.1,  $n = 5$  per group) recipients. Then 12 weeks later, the transplanted BM chimeras were challenged with  $5 \times 10^6$  GFP-transgenic BM cells. The percentage of donor-derived GFP<sup>+</sup> Mac1<sup>+</sup> cells in each mouse was determined by FACS 16 weeks later. Then 16 to 24 weeks after transplantation, chimerism of LSK population in the recipient BM was analyzed. Shown is representative result of 2 independent experiments. For Student *t* tests relative to WT,  $*P < .001$ . BMC, bone marrow cells.

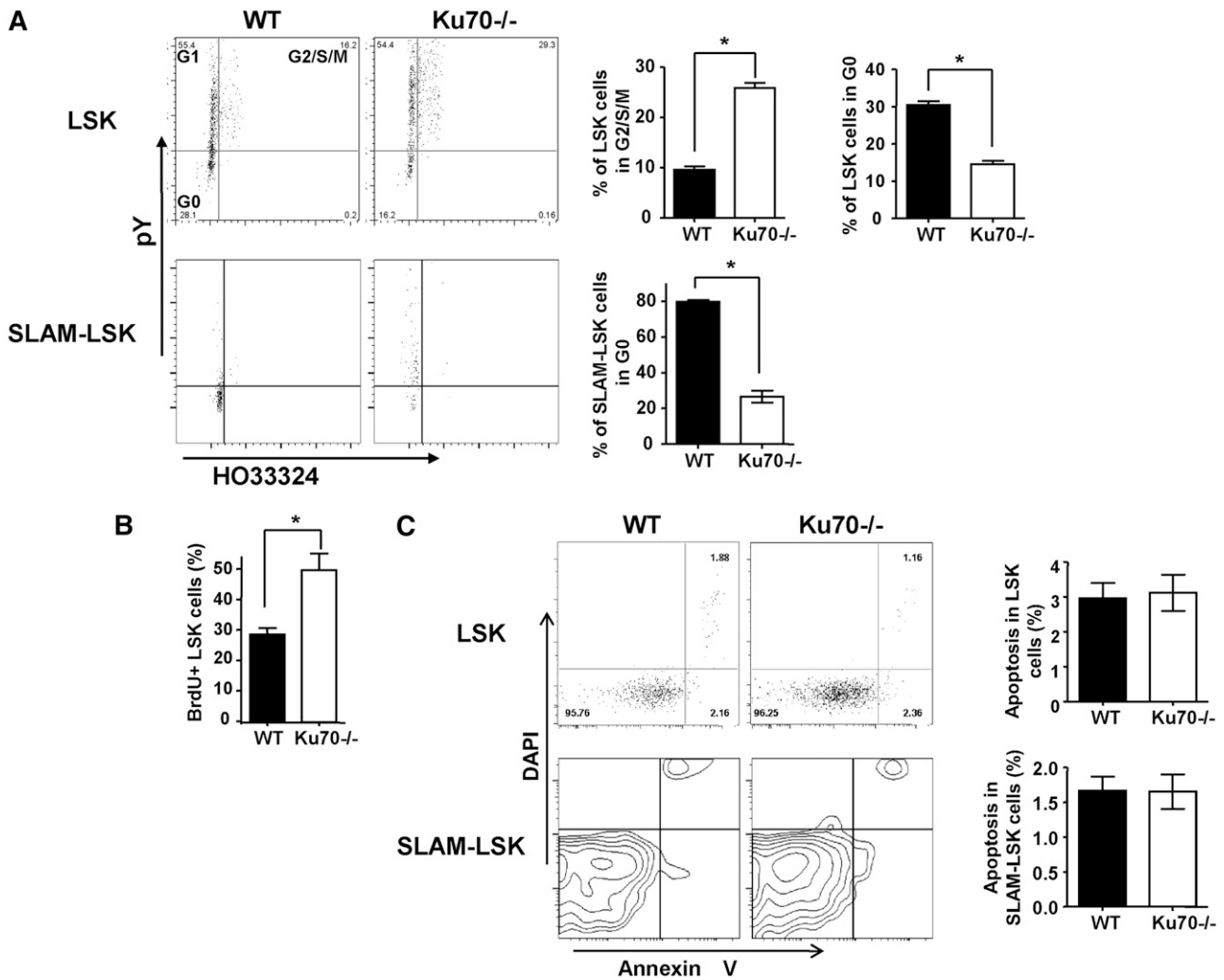


**Figure 3. Proliferation and apoptosis of  $Ku70^{-/-}$  HSCs/progenitors.** (A) BM cells were isolated from 3-month-old  $Ku70^{-/-}$  and WT mice and subjected to FACS analysis after treatment with Hoechst 33342 and Pyronin Y and staining with surface markers. Three separate experiments were performed with 3 to 5 mice per genotype compared. LSK and SLAM-LSK cells were analyzed by Ho33342 contents and pyronin Y intensity, and the proportion of cells in G<sub>2</sub>/S/M or G<sub>0</sub>/G<sub>1</sub> phase was quantitated. Error bars indicate the SD, and significance was determined by a 2-tailed Student *t* test. \**P* < .05. (B) BrdU incorporation. WT (*n* = 5) and  $Ku70^{-/-}$  (*n* = 3) mice were injected and fed with BrdU for 30 hours. BM cells were isolated and BrdU+ proportion within LSK fraction was analyzed. (C) BM cells from  $Ku70^{-/-}$  and WT mice were isolated and subjected to FACS analysis after staining with surface markers along with annexin V and DAPI. The proportion of annexin V-positive (DAPI-negative) cells within the LSK and SLAM-LSK fraction is quantitated. Error bars indicate SD, and significance was determined by a 2-tailed Student *t* test.

SLAM-LSK was decreased significantly in  $Ku70^{-/-}$  mice (Figure 1C). Numerically, the total numbers of LSK, LT-HSC, and SLAM-LSK were significantly decreased in  $Ku70^{-/-}$  mice (Figure 1).

#### Ku70-deficient HSCs have repopulating defects

To assess the self-renewal activity of  $Ku70^{-/-}$  HSCs *in vivo*, non-competitive serial transplantation was performed. Following 2 rounds of transplantation, each after 16 weeks of reconstitution,  $Ku70^{-/-}$  HSCs were not able to rescue the tertiary recipients, whereas WT HSCs were able to support tertiary and quaternary recipients under the same conditions (Figure 2A). Consistent with the loss of reconstitution, a significant reduction in the frequency of LSK cells was also detected in the BM of  $Ku70^{-/-}$  secondary recipients (Figure 2B).

Competitive repopulation assay was also performed. When mixed with WT at 1:1 ratio,  $Ku70^{-/-}$  BM showed a significant competitive repopulation disadvantage, resulting in no detectable contribution to PB leukocyte chimerism even at 8 weeks posttransplantation (Figure 2C).  $Ku70^{-/-}$  LSKs were not detected in the recipient BM

(data not shown). Together, these results demonstrate that  $Ku70^{-/-}$  HSCs have a severely impaired capacity for self-renewal.

#### Lack of Ku70 impairs HSCs BM hematopoietic niche occupancy

BM hematopoietic niche occupancy is an important characteristic of HSCs, which generate long-term hematopoiesis.<sup>40-44</sup> To examine the BM hematopoietic niche occupancy ability of  $Ku70^{-/-}$  HSCs,  $5 \times 10^6$  congenic WT BM cells were transplanted into unconditioned WT or  $Ku70^{-/-}$  mice. As expected, little if any measurable HSC engraftment occurred in WT recipients. In contrast, WT HSCs made a long-term multilineage contribution to hematopoiesis in  $Ku70^{-/-}$  recipients. By 16 weeks after transplantation, more than 80% of LSK cells in the BM and 80% of Mac1<sup>+</sup> cells in the PB were WT donor derived (Figure 2D). In addition, donor-derived lymphoid cells, both T and B cells, are present in the PB of  $Ku70^{-/-}$  recipients (supplemental Figure 2), indicating that the BM microenvironment in  $Ku70^{-/-}$  mice was capable of supporting normal HSC differentiation and lymphoid development.

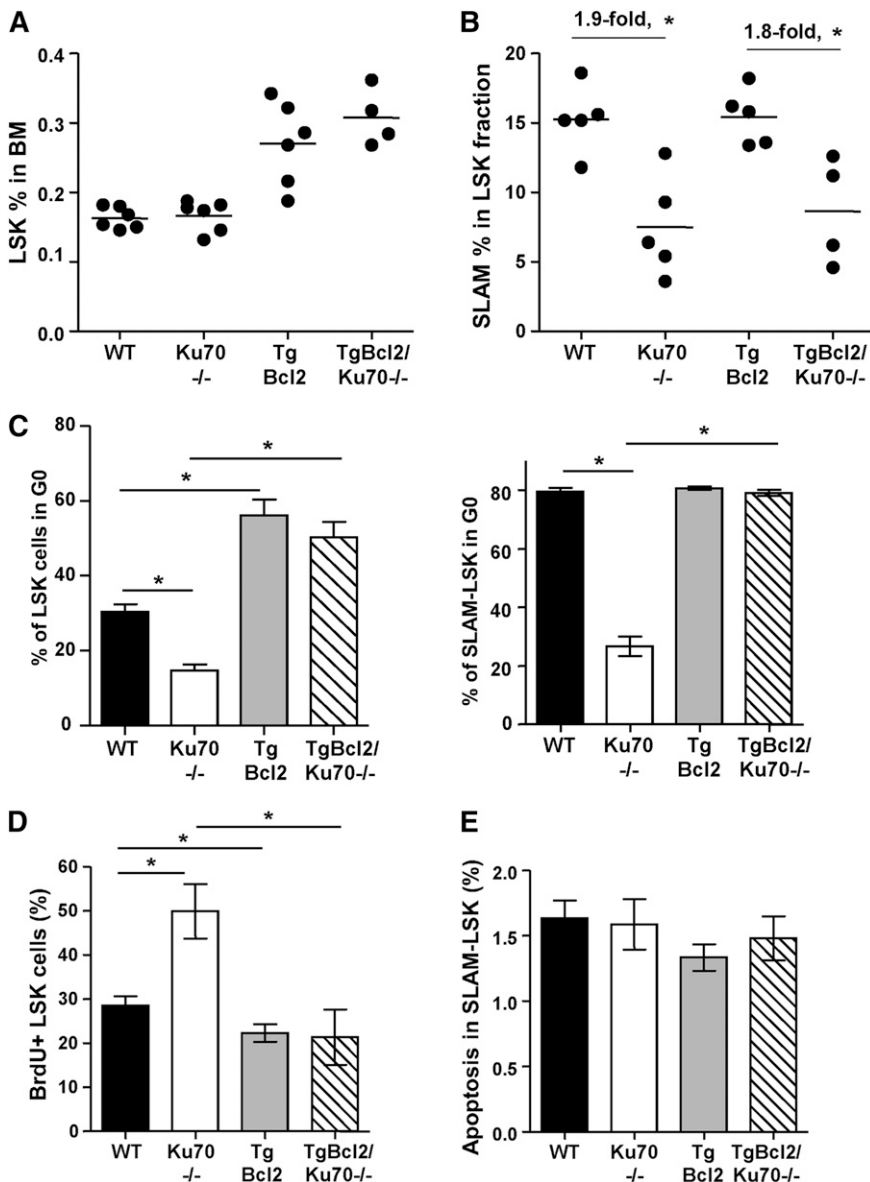


**Figure 4. Overexpression of Bcl2 partially increased HSC/progenitor pools and restored HSC quiescence in *Ku70*<sup>-/-</sup> mice.** (A) BM cells from age-matched WT (*n* = 6), *Ku70*<sup>-/-</sup> (*n* = 6), TgBcl2 (*n* = 5), and TgBcl2/*Ku70*<sup>-/-</sup> (*n* = 4) mice were assayed by multiparameter FACS for proportion of HSC/progenitor populations. Frequency of LSK cells was analyzed. (B) Within the LSK fraction, frequency of SLAM-LSK cells was quantitated. (C) BM cells were isolated from age-matched mice with different genotypes and staining with surface markers after treatment with Hoechst 33342 and pyronin Y. LSK and SLAM-LSK cells were analyzed by HO33342 contents and pyronin Y intensity, and proportion of cells in G<sub>0</sub> phase was quantitated. Three separate experiments were performed with 3 to 5 mice per genotype compared. (D) BrdU incorporation. WT (*n* = 5), *Ku70*<sup>-/-</sup> (*n* = 3), TgBcl2 (*n* = 5), and TgBcl2/*Ku70*<sup>-/-</sup> (*n* = 3) mice were injected and fed with BrdU for 30 hours. BM cells were isolated and BrdU+ proportion within LSK fraction was analyzed. Error bars indicate the SD, and significance was determined by a 2-tailed Student *t* test. \**P* < .05. (E) BM cells from WT, *Ku70*<sup>-/-</sup>, TgBcl2, and TgBcl2/*Ku70*<sup>-/-</sup> mice were isolated and subjected to FACS analysis after staining with surface markers along with annexin V and DAPI. The proportion of annexin V-positive (DAPI-negative) cells within the SLAM-LSK fraction is quantitated.

To exclude the possible effects of the *Ku70*<sup>-/-</sup> BM microenvironment on HSCs, *Ku70*<sup>-/-</sup> or WT BM were transplanted into lethally irradiated WT recipients to generate BM chimeras. A total of  $5 \times 10^6$  GFP transgenic BM were then transplanted into these BM chimeras without additional treatment. GFP BM underwent little engraftment (<2%) in WT recipients, whereas GFP BM established long-term engraftment in *Ku70*<sup>-/-</sup> recipients; 16 weeks after GFP BM transplantation, more than 90% of the BM LSK cells and 75% of the Mac1<sup>+</sup> cells in the PB were GFP<sup>+</sup> (Figure 2E). These results indicate that the functional BM niche occupancy defect of *Ku70*<sup>-/-</sup> HSCs is cell autonomous rather than mediated by the *Ku70*<sup>-/-</sup> BM microenvironment.

#### *Ku70*<sup>-/-</sup> HSCs are less quiescent

We next set out to determine whether the cell-cycle or quiescence status of HSCs was altered by the lack of *Ku70*. Using Hoechst 33324 (Ho) and pyronin Y staining, we identified that  $26.4 \pm 4.2\%$  of LSK cells from *Ku70*<sup>-/-</sup> mice are in the G<sub>2</sub>/S/M phase compared with  $11.5 \pm 3.2\%$  of LSK cells from WT mice (Figure 3A). Only

$14.6 \pm 3.8\%$  of *Ku70*<sup>-/-</sup> LSK cells were in G<sub>0</sub> phase, compared with  $28.3 \pm 6.2\%$  of WT control LSK cells (Figure 3A). Furthermore,  $26.4 \pm 2.3\%$  of *Ku70*<sup>-/-</sup> SLAM-LSK cells were in G<sub>0</sub>, compared with  $79.6 \pm 1.6\%$  of WT cells (Figure 3A). A BrdU incorporation experiment was performed to determine the proliferation of HSCs in *Ku70*<sup>-/-</sup> mice. We found that  $38.6 \pm 4.8\%$  of LSK cells from *Ku70*<sup>-/-</sup> mice are BrdU positive, whereas  $28.4 \pm 3.2\%$  of LSK cells from WT mice are BrdU positive (Figure 3B). *Ku70* BM was more sensitive to fluorouracil (5-FU) treatment in vivo compared with WT BM (supplemental Figure 3), and the increased sensitivity to 5-FU of *Ku70*<sup>-/-</sup> HSCs is likely due to the loss of HSC in the quiescent state, because cells deficient in *Ku70* or the NHEJ pathway were not specifically sensitive to 5-FU.<sup>45</sup> These results showed that loss of *Ku70* in HSCs led to a loss of quiescence and active proliferation.

The effect of *Ku70* on HSC apoptosis at steady state was also examined. Low levels of apoptosis were observed in the LSK and SLAM-LSK fractions from both WT and *Ku70*<sup>-/-</sup> mice (Figure 3C), indicating that *Ku70*<sup>-/-</sup> HSCs/progenitors are not prone to spontaneous apoptosis at steady state.

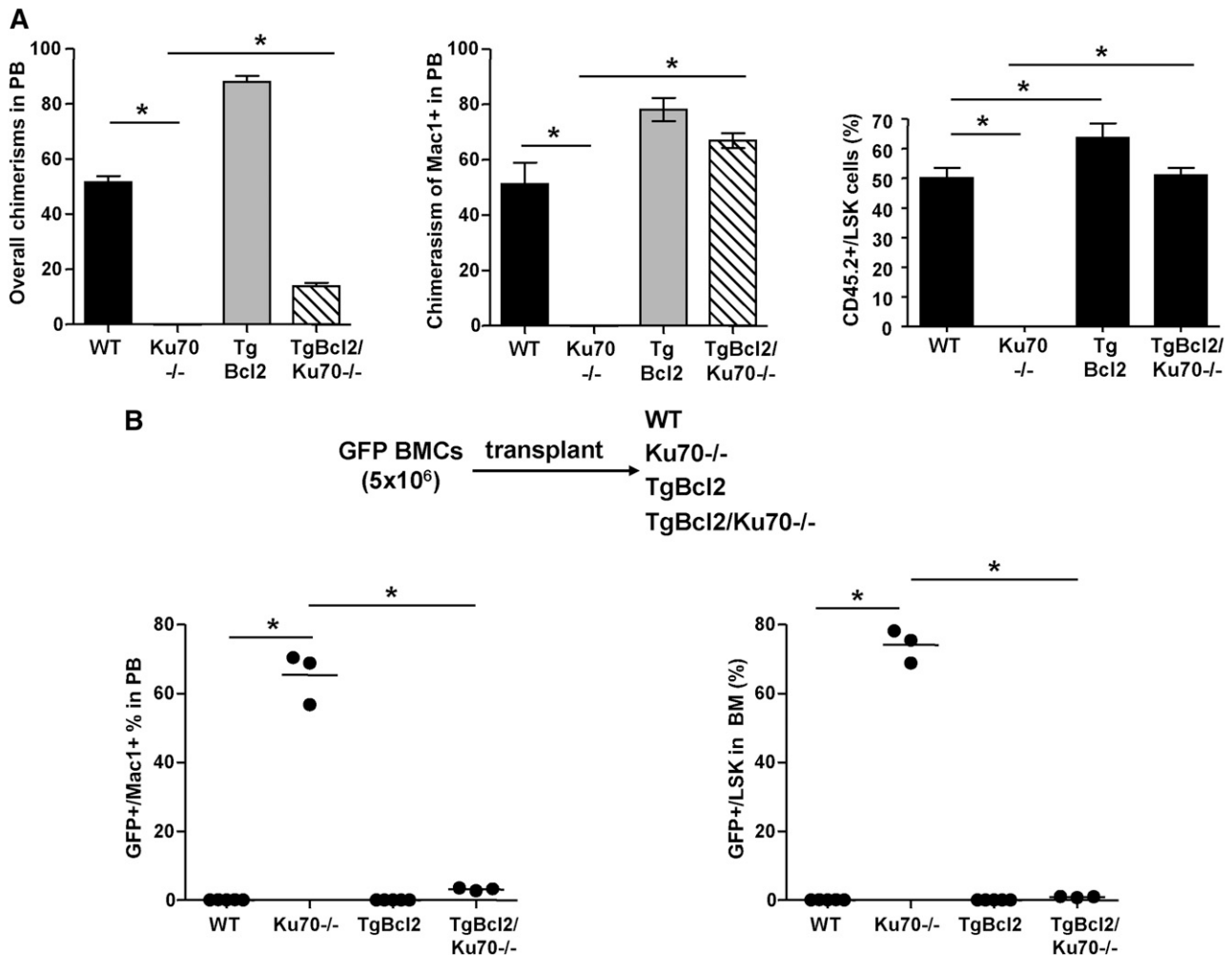


**Figure 5. Overexpression of Bcl2 rescued HSC defects of Ku70<sup>-/-</sup> mice.** (A) Competitive repopulation assay. BM from 3-month-old WT, Ku70<sup>-/-</sup> and TgBcl2, TgBcl2/Ku70<sup>-/-</sup> mice (CD45.2) was isolated and mixed with WT BM (CD45.1) at a 1:1 ratio and transplanted into lethally irradiated WT mice (CD45.1, n = 5 per group). Then 16 weeks posttransplantation, donor chimerisms in the PB and BM LSK cells were analyzed. Similar results were obtained in 2 independent experiments. (B) BM from TgGFP mice was transplanted into 3-month-old mice with different genotypes without any preconditioning. Then 16 weeks posttransplantation, donor chimerisms (GFP+) in the PB and BM LSK cells were quantitated. The number of recipients were WT (n = 5), Ku70<sup>-/-</sup> (n = 3), TgBcl2 (n = 5), and TgBcl2/Ku70<sup>-/-</sup> (n = 3). Error bars indicate the SD, and significance was determined by a 2-tailed Student *t* test. \**P* < .005.

We also examined the growth and apoptosis of Ku70<sup>-/-</sup> HSCs/progenitors *in vitro*. Ku70<sup>-/-</sup> LSK cells display similar expansion rates to those of WT cells (supplemental Figure 4), and Ku70<sup>-/-</sup> LSK cells showed a similar spontaneous apoptosis rate to that of WT cells (supplemental Figure 4).

Together, these results indicate that apoptosis is not the primary cause of the defect in Ku70<sup>-/-</sup> HSCs. Instead, a loss of quiescence contributes to the loss of HSC function in Ku70<sup>-/-</sup> mice.

#### Overexpression of Bcl2 restores HSC quiescence in Ku70-deficient mice

Bcl2 inhibits cell proliferation, and the BM Lin<sup>-</sup> fraction from TgBcl2 mice showed less active proliferation.<sup>32</sup> We hypothesized that Bcl2 overexpression will inhibit HSC proliferation, enhance HSC quiescence, and restore quiescence in Ku70-deficient HSCs. To test this hypothesis, TgBcl2/Ku70<sup>-/-</sup> mice were generated. TgBcl2/Ku70<sup>-/-</sup> mice showed slightly higher BM cellularity and white blood cell counts in PB compared with Ku70<sup>-/-</sup> mice (supplemental Figure 5A-B) and a similar SCID phenotype (with no mature T and B cells) (supplemental Figure 5C), indicating that overexpression of Bcl2 does not rescue V(D)J recombination defect of Ku70<sup>-/-</sup> mice.

The HSC/progenitor pools were analyzed. LSK frequency in the BM of TgBcl2/Ku70<sup>-/-</sup> mice increased by 1.8-fold, compared with Ku70<sup>-/-</sup> mice (Figure 4A), similar with the fold increase in the BM of TgBcl2 mice compared with WT mice (Figure 4A). Interestingly, within the LSK fraction, frequencies of SLAM-LSK cells were not affected by Bcl2 overexpression in WT or Ku70<sup>-/-</sup> mice (Figure 4B). The reduction of LSK and SLAM-LSK numbers in Ku70<sup>-/-</sup> mice was not significantly different on WT and TgBcl2 backgrounds (supplemental Figure 5D). Similarly, Bcl2 overexpression in Tpo<sup>-/-</sup> mice or c-Kit<sup>W41</sup> mice did not restore the primitive HSC pools.<sup>46,47</sup> These results suggest that Bcl2 overexpression did not restore the LT-HSC pool, although it did increase the LSK fraction.

We next analyzed the cell-cycle status/quiescence states and apoptosis of HSCs in mice overexpressing Bcl2. Interestingly, the proportion of LSK cells at G<sub>0</sub> was significantly increased in TgBcl2 compared with WT mice (60.4% ± 3.6% vs 28.3% ± 6.2%) and, more strikingly, the proportion of LSK in G<sub>0</sub> was also significantly improved in TgBcl2/Ku70<sup>-/-</sup> mice compared with Ku70<sup>-/-</sup> mice (59.7% ± 4.6% vs 14.6% ± 3.8%) (Figure 4C). Within the SLAM-LSK fraction, Bcl2 overexpression restored the G<sub>0</sub> proportion in Ku70<sup>-/-</sup> mice (79.1% ± 1.1% vs 26.4% ± 2.3%), though it did not further increase the G<sub>0</sub> proportion in WT mice (80.7% ± 0.6% vs

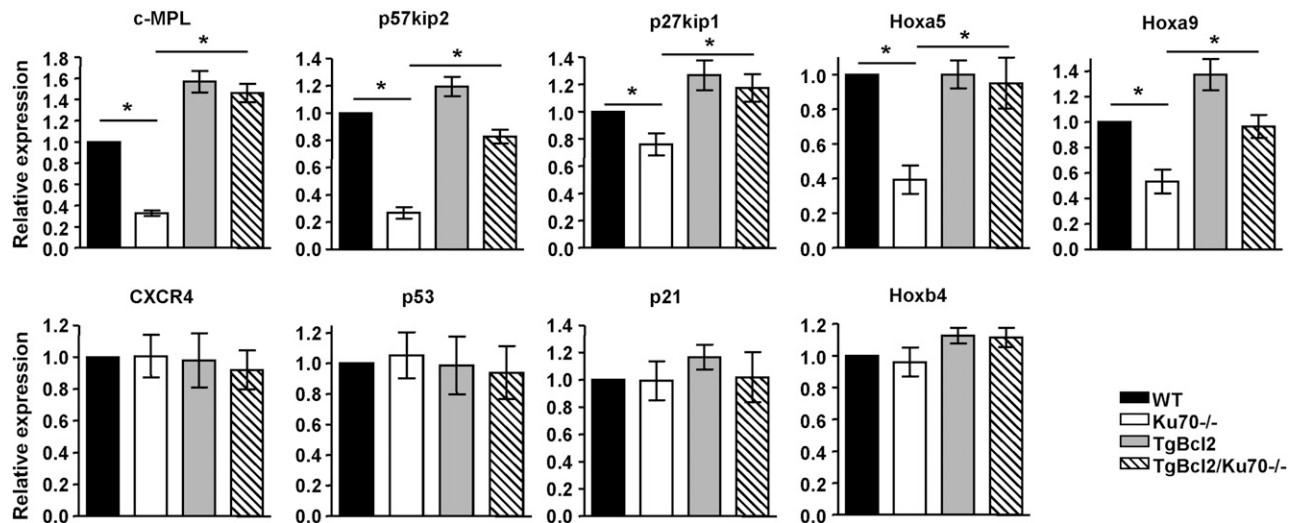


**Figure 6. Expression of quiescence-associated genes in  $Ku70^{-/-}$  HSCs.** BM was isolated from 3 independent groups of WT,  $Ku70^{-/-}$ , and TgBcl2, TgBcl2/ $Ku70^{-/-}$  mice, and LSK cells were sorted before messenger RNA isolation. The relative messenger RNA expression levels of c-Mpl, p57, p27, p53, p21, Hoxa5, Hoxa9, Hoxb4, and CXCR4 were evaluated by quantitative real-time reverse-transcription PCR with endogenous control GAPDH in triplicate. Means from 3 or 4 independent experiments are shown. Error bars indicate SD, and significance was determined by a 2-tailed Student *t* test. \**P* < .05.

79.6% ± 1.6%) (Figure 4C). BrdU incorporation experiments showed that TgBcl2 mice displayed less BrdU incorporation in BM LSK cells compared with WT mice (22.6% ± 4.4% vs 28.4% ± 3.2%), whereas TgBcl2/ $Ku70^{-/-}$  mice showed fewer cycling LSK cells compared with  $Ku70^{-/-}$  mice (23.2% ± 3.2% vs 38.6% ± 4.8%) (Figure 4D). Additionally, spontaneous apoptosis within SLAM-LSK was not significantly altered by Bcl2 overexpression (Figure 4E). These results indicate that overexpression of Bcl2 enhances HSC/progenitor quiescence and restores quiescence in  $Ku70^{-/-}$  HSCs.

#### Overexpression of Bcl2 rescues the HSC defects in $Ku70^{-/-}$ mice

To determine whether overexpression of Bcl2 would rescue the repopulation defect of  $Ku70^{-/-}$  HSCs, competitive repopulation assays were performed. When mixed with WT competitor BM at a 1:1 ratio, TgBcl2 BM cells contributed to ~90% of the overall chimerism and ~80% of Mac1<sup>+</sup> chimerism in the PB. TgBcl2/ $Ku70^{-/-}$  BM cells contributed to ~70% of the Mac1<sup>+</sup> chimerism in the PB. TgBcl2 BM made a significantly higher contribution to BM LSK compared with WT BM (63.46% ± 6.21% vs 50.13% ± 4.33%), and the contribution from TgBcl2/ $Ku70^{-/-}$  BM increased dramatically compared with  $Ku70^{-/-}$  BM (51% ± 2.86% vs 0%) (Figure 5A). These results indicate that overexpression of Bcl2 enhances HSC repopulation activity and can rescue the competitive repopulation defect of  $Ku70^{-/-}$  HSCs. The even greater advantage of TgBcl2 in the PB than in the BM LSK suggests that these cells are actively contributing to hematopoiesis and may also benefit from Bcl2 by prolonging the survival of mature blood cells.

To determine whether overexpression of Bcl2 would rescue the BM hematopoietic niche occupancy defect observed in  $Ku70^{-/-}$  HSCs (Figure 2),  $5 \times 10^6$  BM cells from TgGFP mice were transplanted into each genotype without any conditioning. Similar to the engraftment noted in WT mice, little of any donor engraftment can be detected in TgBcl2 recipient mice. In sharp contrast, whereas donor GFP BM could make significant long-term engraftment in  $Ku70^{-/-}$  mice and contribute to multilineage hematopoiesis, the engraftment of donor WT BM in TgBcl2/ $Ku70^{-/-}$  recipient mice was significantly reduced. By 16 weeks after transplantation, only

about 3% of the Mac1<sup>+</sup> cells in the PB and <2% of BM LSK cells in the TgBcl2/ $Ku70^{-/-}$  recipients are GFP<sup>+</sup> (Figure 5B). This result indicates that Bcl2 overexpression rescues the BM hematopoietic niche occupancy defect of  $Ku70^{-/-}$  HSCs.

Our results demonstrate that Bcl2 overexpression rescued the HSC maintenance defects in  $Ku70^{-/-}$  mice mainly by restoration of HSC quiescence, in addition to the enhanced survival. To investigate the mechanisms by which Ku70 and Bcl2 regulate HSC quiescence, expression of several HSC function- or quiescence-related genes were examined in sorted BM LSK cells by real-time reverse-transcription PCR. We found that in the  $Ku70^{-/-}$  LSK cells, expression of c-MPL, p57<sup>kip2</sup> was downregulated by about 3-fold and that expression of p27, Hoxa5, Hoxa9 was also downregulated (Figure 6). Consistent with the biological activity noted, overexpression of Bcl2 restores the expression of c-MPL, p57 to the level of WT LSK cells and also that of p27, Hoxa5, Hoxa9 (Figure 6). The expression of p53, p21, Hoxb4, CXCR4 was not significantly altered among each genotype, suggesting that changes in these functions are not critical to the observed defect of Bcl2 effect. Our results suggest that multiple pathways are involved in the loss of HSC quiescence in  $Ku70^{-/-}$  mice. Bcl2 rescue of the  $Ku70^{-/-}$  HSC quiescence defect is enough to compensate for many of these pathway changes.

#### Overexpression of Bcl2 does not restore the DNA-repair defect of $Ku70^{-/-}$ HSCs

Our results have demonstrated that overexpression of Bcl2 restored HSC maintenance in  $Ku70^{-/-}$  mice and that Ku70 is essential for DNA repair. However, it is important to examine whether overexpression of Bcl2 would restore DNA repair capacity in  $Ku70^{-/-}$  HSCs. In response to 2 Gy radiation,  $Ku70^{-/-}$  BM cells failed to grow and form colonies in a colony-forming unit assay and Bcl2 overexpression increased the resistance to radiation in TgBcl2 BM, but not TgBcl2/ $Ku70^{-/-}$  BM (Figure 7A). Radiosensitivity of HSCs was also examined in primary recipients reconstituted with different-genotype BM. Although WT and TgBcl2 BM recipient mice survived 2 Gy radiation well beyond 2 months, all  $Ku70^{-/-}$  BM and TgBcl2/ $Ku70^{-/-}$  BM recipient mice died within 1 month (Figure 7B).

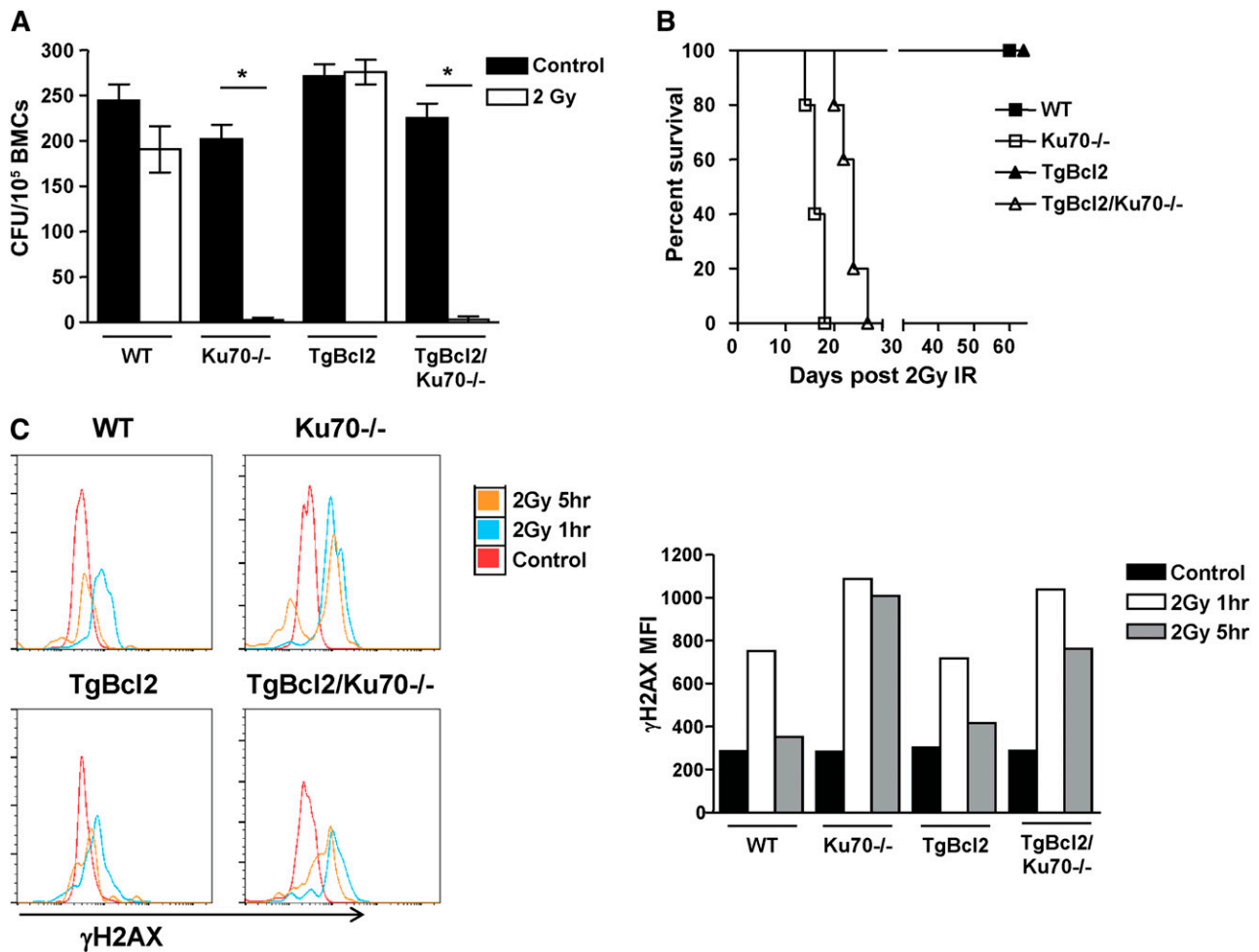


**Figure 7. Overexpression of Bcl2 did not restore DNA repair capacity in Ku70<sup>-/-</sup> HSCs.** (A) Three-month-old WT, Ku70<sup>-/-</sup>, TgBcl2, and TgBcl2/Ku70<sup>-/-</sup> mice were irradiated with 2 Gy. BM cells were isolated and plated in methylcellulose in the presence of interleukin-3, interleukin-6, and stem cell factor. Colony-forming units were counted 14 days later. Shown is the representative result of 2 independent experiments. Error bars indicate SD, and significance was determined by a 2-tailed Student *t* test. \**P* < .001. (B) BM cells from 3-month-old WT, Ku70<sup>-/-</sup>, TgBcl2 and TgBcl2/Ku70<sup>-/-</sup> mice were transplanted into lethally irradiated BoyJ recipients. Then 12 weeks posttransplantation, the recipients were irradiated with 2 Gy radiation and survival of the recipients was monitored (*n* = 5 per group). (C) Three-month-old WT, Ku70<sup>-/-</sup>, TgBcl2, and TgBcl2/Ku70<sup>-/-</sup> mice were irradiated with 2 Gy and at each time point BM cells were isolated and analyzed by FACS to assess the levels of γH2AX in the SLAM-LSK fraction. Shown is the representative result of 2 independent experiments. CFU, colony-forming units; IR, irradiation.

Next, we examined γH2AX levels in the SLAM-LSK fraction of mice after 2 Gy radiation. At steady state, γH2AX levels in HSCs with 4 genotypes were similar. In response to 2 Gy radiation, γH2AX levels increased in WT HSCs at 1 hour and resolved by 5 hours, whereas higher levels of γH2AX were observed in Ku70<sup>-/-</sup> HSCs at 1 hour and persisted at 5 hours. Bcl2 overexpression did not impact the γH2AX levels in TgBcl2 or TgBcl2/Ku70<sup>-/-</sup> HSCs (Figure 7C). In addition, HSCs diminished in the BM of Ku70<sup>-/-</sup> mice 24 hours after 2Gy radiation (supplemental Figure 6). These results indicated that Ku70<sup>-/-</sup> HSCs are hypersensitive to radiation and that overexpression of Bcl2 did not restore DNA repair capacity and protect Ku70<sup>-/-</sup> HSCs from radiation.

## Discussion

Our studies demonstrate that Ku70 is essential for HSC maintenance. Lack of Ku70 results in loss of HSC quiescence and HSC maintenance, including self-renewal, competitive repopulation, and BM hematopoietic niche occupancy activities. Furthermore, overexpression of Bcl2 in

HSCs promotes quiescence, restores quiescence in Ku70<sup>-/-</sup> HSCs, and rescues the HSC maintenance defects in Ku70<sup>-/-</sup> mice.

### HSC apoptosis and proliferation in Ku70<sup>-/-</sup> mice

Apoptosis, proliferation, and interaction with BM niche are important factors for HSC maintenance. Ku70<sup>-/-</sup> HSCs/progenitors display comparable apoptosis rates with WT control at steady state (Figure 3) and after in vitro culture (our unpublished results), indicating that Ku70<sup>-/-</sup> HSCs are not prone to spontaneous apoptosis. HSCs deficient in caspase-3 are resistant to apoptosis but defective in maintenance, suggesting that apoptosis is not the primary cause of HSC defects.<sup>48</sup> Although we cannot definitely rule out the possible apoptosis differences in vivo, we conclude that HSC defects of Ku70<sup>-/-</sup> mice are not primarily due to apoptosis.

Instead, we found that Ku70<sup>-/-</sup> HSC/progenitors lose quiescence (Figure 3) and Lig4<sup>Y288C</sup> LSKs also showed increased BrdU incorporation.<sup>22</sup> These results together suggested that deficiency of NHEJ in HSCs leads to increased proliferation. However, mouse embryonic fibroblasts deficient in Ku70 or Lig4 display decreased proliferation.<sup>21,22</sup> It is likely that the HSC response to proliferative



signals in the absence of DNA repair may be regulated by both hematopoietic and quiescence signals.

Although some cell-cycle regulators have been shown to be directly involved in G<sub>0</sub> maintenance, the cooperation of several cell-cycle regulators may also be required for quiescence regulation.<sup>49-51</sup> We observed decreased expression of p27 and p57, but not p53 and p21, in Ku70<sup>-/-</sup> HSCs/progenitors (Figure 6). Several cell-cell interaction signaling pathways have also been implicated in the maintenance of HSC quiescence.<sup>47,52,53</sup> Here, the expression of c-Mpl and its target gene p57 was downregulated in Ku70<sup>-/-</sup> HSCs, suggesting that the c-Mpl signaling pathway may mediate the quiescence regulation by Ku70 in HSCs. However, it is not clear whether decreased c-Mpl signaling is a direct target of Ku70 loss or a concurrent phenotype of loss of HSC quiescence. More likely, Ku70 or NHEJ regulates quiescence and these mediators act downstream. Tpo can enhance DNA repair in HSCs by stimulating DNA PKcs in response to radiation,<sup>54</sup> and in Ku70<sup>-/-</sup> HSC/progenitors, the decreased expression of Tpo receptor (c-Mpl), the absence of Ku70, and the reduced DNA PKcs activity may synergistically lead to hypersensitivity to radiation (Figure 7; supplemental Figure 6).

### The role of Bcl2 in HSC maintenance

Previous results indicate that Bcl2 enhances HSC function by protecting HSCs against apoptosis.<sup>33,55</sup> However, human CD34<sup>+</sup> cord blood cells overexpressing Bcl2 displayed better transplantability compared with cells overexpressing a mutant p53, which is also defective in inducing apoptosis.<sup>56</sup> In addition, when the impact of p53 loss and Bcl2 overexpression on a NUP98-HOXD13 (NHD13)-induced myelodysplastic syndrome mouse model was examined, overexpression of Bcl2 delayed AML transition, whereas deletion of p53 accelerated AML transition.<sup>57,58</sup> These findings suggest Bcl2 may have more activity in HSCs beyond simply antiapoptosis. Our results showed that overexpression of Bcl2 results in increased HSC quiescence and decreased proliferation (Figure 4). Strikingly, overexpression of Bcl2 rescues the Ku70<sup>-/-</sup> HSC maintenance defects, including competitive repopulation and BM hematopoietic niche occupancy (Figure 5). Ku70<sup>-/-</sup> HSCs are not prone to spontaneous apoptosis but lose quiescence at steady state (Figure 3). Overexpression of Bcl2 restores the quiescence in Ku70<sup>-/-</sup> HSCs, and in so doing, Bcl2 plays an essential role in the rescue of Ku70<sup>-/-</sup> HSC maintenance defects.

### DNA-repair pathways and HSC maintenance

DNA-repair activity in HSCs has not been well studied. Although endogenous DNA damage may exist in the HSC compartment in DNA-repair-deficient mice, whether this damage directly impairs HSC function is not clear. In Ku70<sup>-/-</sup> HSCs, the endogenous levels of

DNA damage, determined by  $\gamma$ H2Ax, was not significantly different from WT cells (Figure 7C). Our results also showed that overexpression of Bcl2 in Ku70<sup>-/-</sup> HSCs can rescue the HSC defects in Ku70<sup>-/-</sup> mice (Figure 5), whereas it did not restore DNA-repair capacity in Ku70<sup>-/-</sup> HSCs (Figure 7; supplemental Figure 5C). In human tumor cell lines, overexpression of Bcl2 negatively regulates DNA-repair pathways, including NHEJ.<sup>59</sup> These results suggest that overexpression of Bcl2 can override the defects caused by DNA-repair deficiency in restoring HSC function. It is tempting to speculate that the endogenous DNA damage in Ku70<sup>-/-</sup> cells may not impair HSC function directly but rather impairs HSCs indirectly by reducing quiescence. This is reinforced by the finding that HSC quiescence is restored by overexpression of Bcl2, restoring HSC function without regaining NHEJ DNA-repair capacity. Although we further hypothesize that HSCs, in the absence of NHEJ, enter the cell cycle to repair DSBs by homologous recombination as at least one explanation of loss of quiescence, more studies are required to investigate the mechanisms by which loss of the NHEJ pathway results in loss of HSC quiescence.

### Acknowledgments

This research was supported by the Cytometry and Imaging Microscopy Core Facility of the Case Comprehensive Cancer Center (P30 CA43703) and by National Institutes of Health (National Cancer Institute) grant R01CA063193.

### Authorship

Contribution: Y.Q. designed and performed the experiments and prepared the manuscript; Z.W. designed and performed the experiments; K.D.B. designed the experiments and interpreted the results; and S.L.G. designed the experiments, interpreted the results, and prepared the manuscript.

Conflict-of-interest disclosure: The authors declare no competing financial interests.

The current affiliation for Z.W. and K.D.B. is Department of Pediatrics, Aflac Cancer and Blood Disorders Center, Emory University School of Medicine.

Correspondence: Stanton L. Gerson, Case Comprehensive Cancer Center, National Center for Regenerative Medicine, Seidman Cancer Center, University Hospitals Case Medical Center and Case Western Reserve University, 11100 Euclid Ave, Wearn Room 151, Cleveland, OH 44106-5065; e-mail: slg5@case.edu.

### References

- Park Y, Gerson SL. DNA repair defects in stem cell function and aging. *Annu Rev Med*. 2005;56:495-508.
- He S, Nakada D, Morrison SJ. Mechanisms of stem cell self-renewal. *Annu Rev Cell Dev Biol*. 2009;25:377-406.
- Jackson SP, Bartek J. The DNA-damage response in human biology and disease. *Nature*. 2009;461(7267):1071-1078.
- Lombard DB, Chua KF, Mostoslavsky R, Franco S, Gostissa M, Alt FW. DNA repair, genome stability, and aging. *Cell*. 2005;120(4):497-512.
- Rossi DJ, Jamieson CH, Weissman IL. Stem cells and the pathways to aging and cancer. *Cell*. 2008;132(4):681-696.
- Friedberg EC. DNA damage and repair. *Nature*. 2003;421(6921):436-440.
- Niedernhofer LJ. DNA repair is crucial for maintaining hematopoietic stem cell function. *DNA Repair (Amst)*. 2008;7(3):523-529.
- Li L, Clevers H. Coexistence of quiescent and active adult stem cells in mammals. *Science*. 2010;327(5965):542-545.
- Orford KW, Scadden DT. Deconstructing stem cell self-renewal: genetic insights into cell-cycle regulation. *Nat Rev Genet*. 2008;9(2):115-128.
- Raaijmakers MH, Scadden DT. Divided within: heterogeneity within adult stem cell pools. *Cell*. 2008;135(6):1006-1008.
- Wilson A, Laurenti E, Oser G, et al. Hematopoietic stem cells reversibly switch from dormancy to self-renewal during homeostasis and repair. *Cell*. 2008;135(6):1118-1129.
- Wilson A, Laurenti E, Trumpp A. Balancing dormant and self-renewing hematopoietic stem cells. *Curr Opin Genet Dev*. 2009;19(5):461-468.
- Pietras EM, Warr MR, Passegué E. Cell cycle regulation in hematopoietic stem cells. *J Cell Biol*. 2011;195(5):709-720.
- Rossi L, Lin KK, Boles NC, et al. Less is more: unveiling the functional core of hematopoietic stem cells through knockout mice. *Cell Stem Cell*. 2012;11(3):302-317.

15. Mills KD, Ferguson DO, Alt FW. The role of DNA breaks in genomic instability and tumorigenesis. *Immunol Rev*. 2003;194:77-95.
16. Bassing CH, Alt FW. The cellular response to general and programmed DNA double strand breaks. *DNA Repair (Amst)*. 2004;3(8-9):781-796.
17. Hartlerode AJ, Scully R. Mechanisms of double-strand break repair in somatic mammalian cells. *Biochem J*. 2009;423(2):157-168.
18. Collis SJ, DeWeese TL, Jeggo PA, Parker AR. The life and death of DNA-PK. *Oncogene*. 2005;24(6):949-961.
19. Lieber MR. The mechanism of double-strand DNA break repair by the nonhomologous DNA end-joining pathway. *Annu Rev Biochem*. 2010;79:181-211.
20. Gao Y, Chaudhuri J, Zhu C, Davidson L, Weaver DT, Alt FW. A targeted DNA-PKcs-null mutation reveals DNA-PK-independent functions for KU in V(D)J recombination. *Immunity*. 1998;9(3):367-376.
21. Gu Y, Seidl KJ, Rathbun GA, et al. Growth retardation and leaky SCID phenotype of Ku70-deficient mice. *Immunity*. 1997;7(5):653-665.
22. Nijnik A, Woodbine L, Marchetti C, et al. DNA repair is limiting for haematopoietic stem cells during ageing. *Nature*. 2007;447(7145):686-690.
23. Nussenzweig A, Chen C, da Costa Soares V, Sanchez M, Sokol K, Nussenzweig MC, Li GC. Requirement for Ku80 in growth and immunoglobulin V(D)J recombination. *Nature*. 1996;382(6591):551-555.
24. Rooney S, Sekiguchi J, Zhu C, et al. Leaky Scid phenotype associated with defective V(D)J coding end processing in Artemis-deficient mice. *Mol Cell*. 2002;10(6):1379-1390.
25. Mohrin M, Bourke E, Alexander D, et al. Hematopoietic stem cell quiescence promotes error-prone DNA repair and mutagenesis. *Cell Stem Cell*. 2010;7(2):174-185.
26. Rossi DJ, Seita J, Czechowicz A, Bhattacharya D, Bryder D, Weissman IL. Hematopoietic stem cell quiescence attenuates DNA damage response and permits DNA damage accumulation during aging. *Cell Cycle*. 2007;6(19):2371-2376.
27. Tsujimoto Y, Finger LR, Yunis J, Nowell PC, Croce CM. Cloning of the chromosome breakpoint of neoplastic B cells with the t(14;18) chromosome translocation. *Science*. 1984;226(4678):1097-1099.
28. Chipuk JE, Moldoveanu T, Llambi F, Parsons MJ, Green DR. The BCL-2 family reunion. *Mol Cell*. 2010;37(3):299-310.
29. Youle RJ, Strasser A. The BCL-2 protein family: opposing activities that mediate cell death. *Nat Rev Mol Cell Biol*. 2008;9(1):47-59.
30. Kelly PN, Strasser A. The role of Bcl-2 and its pro-survival relatives in tumorigenesis and cancer therapy. *Cell Death Differ*. 2011;18(9):1414-1424.
31. Llambi F, Green DR. Apoptosis and oncogenesis: give and take in the BCL-2 family. *Curr Opin Genet Dev*. 2011;21(1):12-20.
32. Domen J, Cheshier SH, Weissman IL. The role of apoptosis in the regulation of hematopoietic stem cells: Overexpression of Bcl-2 increases both their number and repopulation potential. *J Exp Med*. 2000;191(2):253-264.
33. Domen J, Gandy KL, Weissman IL. Systemic overexpression of BCL-2 in the hematopoietic system protects transgenic mice from the consequences of lethal irradiation. *Blood*. 1998;91(7):2272-2282.
34. Linette GP, Li Y, Roth K, Korsmeyer SJ. Cross talk between cell death and cell cycle progression: BCL-2 regulates NFAT-mediated activation. *Proc Natl Acad Sci USA*. 1996;93(18):9545-9552.
35. Vaux DL, Cory S, Adams JM. Bcl-2 gene promotes haemopoietic cell survival and cooperates with c-myc to immortalize pre-B cells. *Nature*. 1988;335(6189):440-442.
36. Janumyan YM, Sansam CG, Chattopadhyay A, et al. Bcl-xL/Bcl-2 coordinately regulates apoptosis, cell cycle arrest and cell cycle entry. *EMBO J*. 2003;22(20):5459-5470.
37. Zinkel S, Gross A, Yang E. BCL2 family in DNA damage and cell cycle control. *Cell Death Differ*. 2006;13(8):1351-1359.
38. Huang X, Darzynkiewicz Z. Cytometric assessment of histone H2AX phosphorylation: a reporter of DNA damage. *Methods Mol Biol*. 2006;314:73-80.
39. Ouyang H, Nussenzweig A, Kurimasa A, et al. Ku70 is required for DNA repair but not for T cell antigen receptor gene recombination in vivo. *J Exp Med*. 1997;186(6):921-929.
40. Voog J, Jones DL. Stem cells and the niche: a dynamic duo. *Cell Stem Cell*. 2010;6(2):103-115.
41. Papayannopoulou T, Scadden DT. Stem-cell ecology and stem cells in motion. *Blood*. 2008;111(8):3923-3930.
42. Wilson A, Trumpp A. Bone-marrow haematopoietic-stem-cell niches. *Nat Rev Immunol*. 2006;6(2):93-106.
43. Zhang J, Li L. Stem cell niche: microenvironment and beyond. *J Biol Chem*. 2008;283(15):9499-9503.
44. Qing Y, Lin Y, Gerson SL. An intrinsic BM hematopoietic niche occupancy defect of HSC in scid mice facilitates exogenous HSC engraftment. *Blood*. 2012;119(7):1768-1771.
45. Wyatt MD, Wilson DM III. Participation of DNA repair in the response to 5-fluorouracil. *Cell Mol Life Sci*. 2009;66(5):788-799.
46. Thorén LA, Liuba K, Bryder D, et al. Kit regulates maintenance of quiescent hematopoietic stem cells. *J Immunol*. 2008;180(4):2045-2053.
47. Qian H, Buza-Vidas N, Hyland CD, et al. Critical role of thrombopoietin in maintaining adult quiescent hematopoietic stem cells. *Cell Stem Cell*. 2007;1(6):671-684.
48. Janzen V, Fleming HE, Riedt T, et al. Hematopoietic stem cell responsiveness to exogenous signals is limited by caspase-3. *Cell Stem Cell*. 2008;2(6):584-594.
49. Walkley CR, Fero ML, Chien WM, Purton LE, McArthur GA. Negative cell-cycle regulators cooperatively control self-renewal and differentiation of haematopoietic stem cells. *Nat Cell Biol*. 2005;7(2):172-178.
50. Zou P, Yoshihara H, Hosokawa K, et al. p57(Kip2) and p27(Kip1) cooperate to maintain hematopoietic stem cell quiescence through interactions with Hsc70. *Cell Stem Cell*. 2011;9(3):247-261.
51. Matsumoto A, Takeishi S, Kanie T, et al. p57 is required for quiescence and maintenance of adult hematopoietic stem cells. *Cell Stem Cell*. 2011;9(3):262-271.
52. Arai F, Hirao A, Ohmura M, et al. Tie2/angiopoietin-1 signaling regulates hematopoietic stem cell quiescence in the bone marrow niche. *Cell*. 2004;118(2):149-161.
53. Yoshihara H, Arai F, Hosokawa K, et al. Thrombopoietin/MPL signaling regulates hematopoietic stem cell quiescence and interaction with the osteoblastic niche. *Cell Stem Cell*. 2007;1(6):685-697.
54. de Laval B, Pawlikowska P, Petit-Cocault L, et al. Thrombopoietin-increased DNA-PK-dependent DNA repair limits hematopoietic stem and progenitor cell mutagenesis in response to DNA damage. *Cell Stem Cell*. 2013;12(1):37-48.
55. Matsuzaki Y, Nakayama K, Nakayama K, Tomita T, Isoda M, Loh DY, Nakauchi H. Role of bcl-2 in the development of lymphoid cells from the hematopoietic stem cell. *Blood*. 1997;89(3):853-862.
56. Milyavsky M, Gan OI, Trotter M, et al. A distinctive DNA damage response in human hematopoietic stem cells reveals an apoptosis-independent role for p53 in self-renewal. *Cell Stem Cell*. 2010;7(2):186-197.
57. Xu H, Menendez S, Schlegelberger B, et al. Loss of p53 accelerates the complications of myelodysplastic syndrome in a NUP98-HOXD13-driven mouse model. *Blood*. 2012;120(15):3089-3097.
58. Slape CI, Saw J, Jowett JB, Aplan PD, Strasser A, Jane SM, Curtis DJ. Inhibition of apoptosis by BCL2 prevents leukemic transformation of a murine myelodysplastic syndrome. *Blood*. 2012;120(12):2475-2483.
59. Wang Q, Gao F, May WS, Zhang Y, Flagg T, Deng X. Bcl2 negatively regulates DNA double-strand-break repair through a nonhomologous end-joining pathway. *Mol Cell*. 2008;29(4):488-498.